Journal of Electroanalytical Chemistry 638 (2010) 51–58

Contents lists available at ScienceDirect

Journal of Electroanalytical Chemistry

journal homepage: www.elsevier.com/locate/jelechem

EIS characterization of tantalum and niobium oxide films based on a modification of the point defect model

Román Cabrera-Sierra [a,*], José Manuel Hallen [b], Jorge Vazquez-Arenas [c], Gerardo Vázquez [d], Ignacio González [d]

[a] Instituto Politécnico Nacional, Escuela Superior de Ingeniería Química e Industrias Extractivas, Academia de Química Analítica. UPALM Ed. Z5, CP 07738, DF, Mexico
[b] Instituto Politécnico Nacional, Escuela Superior de Ingeniería Química e Industrias Extractivas, Departamento de Ingeniería Metalúrgica. UPALM Ed. 7, CP 07738, DF, Mexico
[c] Chemical Engineering Department, University of Waterloo, 200 University Avenue West, Waterloo, Ontario, Canada N2L 3G1
[d] Universidad Autónoma Metropolitana, Departamento de Química. Apdo. Postal 55-534, CP 09340, DF, Mexico

A R T I C L E   I N F O

Article history:
Received 25 July 2009
Received in revised form 10 October 2009
Accepted 14 October 2009
Available online 20 October 2009

Keywords:
Oxygen vacancy
Hydroxyl vacancy
PDM
Passive films
Blistering

A B S T R A C T

Electrochemical impedance spectroscopy (EIS) studies were performed to analyze the passive properties of tantalum and niobium oxides films potentiostatically formed in a 0.1 M KOH solution. The quantitative characterization of these passive materials was carried out through a transfer function previously developed by our research group, which is based on the point defect model (PDM) framework considering the formation of molecular hydrogen. According to the PDM prediction criteria, Ta_2O_5 and Nb_2O_5 films exhibited an inherent *n*-type semiconductor behavior, which was confirmed by the parameters obtained from the fit to the transfer function. The diffusion coefficients of the oxygen vacancies were $0.53 \pm 0.14 \times 10^{-16}$ and $2.18 \pm 0.14 \times 10^{-16}$ cm^2 s^{-1}, for Ta_2O_5 and Nb_2O_5, respectively. And a slight increase of the corresponding hydroxyl vacancies diffusion (2.73 ± 0.02 and $2.23 \pm 0.65 \times 10^{-16}$ cm^2 s^{-1}) was obtained, suggesting the favorable diffusion of these defects due to the alkaline conditions.

© 2009 Elsevier B.V. All rights reserved.

1. Introduction

Metals and alloys passivity is an important phenomenon in the material science since it is the key to increase the corrosion resistance of metals. The blistering damage is an important occurrence observed on passive oxides, because it has been experimentally reported as one of the possible reasons provoking the breakdown of the films, which have been related to localized corrosion pitting [1,2]. The blistering damage has been observed in metals such as aluminum, zirconium, niobium in aqueous solutions; it has also been suggested that it may occur in the presence or absence of halide ions [1,2]. The breakdown of oxide films may be promoted by the formation of molecular hydrogen at the metal–film interface, when a critical condition of pressure is reached. Experimental evidence for this phenomenon has been reported in the literature for different electrochemical interfaces [1–17].

In a previous paper [18], we have extensively described different experimental results reported in the literature related to a hydration mechanism of passive oxide films involving the migration of OH^- ions between oxygen vacancies to form oxyhydroxide or hydroxide phases. In this work, we make a proposal considering that the hydration of the passive films not only modifies the structure and composition of the film, but also contributes to non-uniform corrosion or pitting due to the creation of film stress and the generation of hydrogen gas at the metal–oxide interface.

A schematic description of the latter model is sketched in Fig. 1, previously reported by Cabrera-Sierra et al. [18]. This figure represents the formation and annihilation processes of different types of defects subjected to diffusion across the passive films. These films are modeled in this study considering that are comprised by a double layer structure: an inner poorly hydrated oxide and an outer hydroxide phase. The metal–film interface does not involve an uniform metal–oxide interface because of the incorporation of some hydroxyl ions. On the same hand, the inner layer is a highly defective semiconductor (either *p*- or *n*-type), where the electronic conduction across it is described by the transport of vacancies acting as electronic dopants. To this concern, on *p*-type oxide films, the majority of carriers are cation vacancies ($V_M^{\chi'}$), and for *n*-type, the majority of carriers are oxygen vacancies ($V_O^{\bullet\bullet}$) and/or interstitial metallic ions ($M_i^{\chi+}$) [18–22]. For both cases (*p*- and *n*-type), the model considers the formation and/or annihilation of hydroxyl vacancies ($V_{OH}^{\bullet}$, reactions 3b and 6b), at the metal–film and film–solution interfaces, respectively. Molecular hydrogen can be formed by a recombination process (i.e. Tafel mechanism) owing to diffusion of hydroxyl ions across the oxide films, where mono-atomic hydrogen is trapped due to reduction reactions at the metal–oxide interface. Fluxes of cation, oxygen and hydroxyl vacancies are

* Corresponding author. Tel.: +52 55 57296000x55137.
E-mail address: roma_ipn@yahoo.com (R. Cabrera-Sierra).

0022-0728/$ - see front matter © 2009 Elsevier B.V. All rights reserved.
doi:10.1016/j.jelechem.2009.10.021

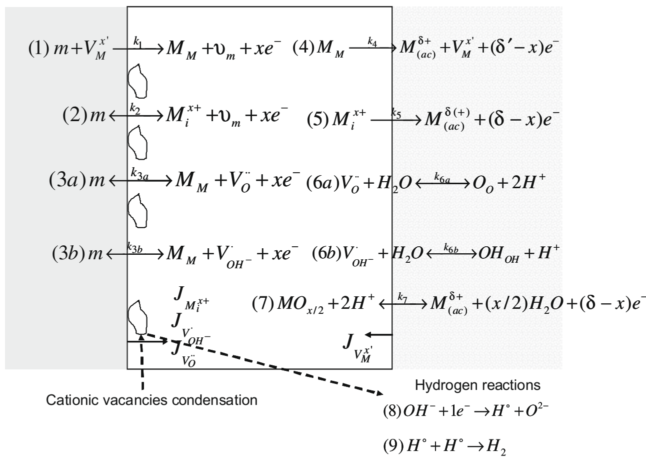

Fig. 1. Schematic representation of the passive state, within the framework of the PDM and considering the formation of molecular hydrogen. υ_m is a vacancy in metal phase, $V_M^{\chi'}$, $V_O^{\cdot\cdot}$ and $V_{OH}^{\cdot}$ are the cation, oxygen and hydroxyl vacancies, respectively. $M_i^{\chi+}$ is an interstitial cation, M_M is a metal cation in a cation site and O_O is a oxygen ion in anion site, while OH_{OH} is a hydroxyl ion in hydroxyl site and $M^{\delta+}(ac)$ is a cation in solution. This figure has been previously reported by Cabrera-Sierra et al. [18].

described by the arrows direction indicated in Fig. 1. More details about this model can be found in Ref. [18]. Kroger–Vink notation used in Fig. 1 has been described in detail in the literature [19–22].

From the model presented in Fig. 1, the corresponding transfer functions were derived [18] for *p*- and *n*-type semiconductor films considering that the total impedance is dominated by this barrier layer. Those corresponding for the *n*-type are shown in Eqs. (1)–(5).

$$(Z_T - R_s)^{-1} = j\omega C_p + Z_f^{-1} \tag{1}$$

Z_T and R_s are the overall impedance and the solution resistance, respectively. C_p is the interfacial capacitance and Z_f is the overall faradaic impedance, which is given by the expression:

$$Z_f = Z_{fo} + Z_{fh} \tag{2}$$

where Z_{fo} and Z_{fh} are the faradaic impedances of oxygen and hydroxyl ion vacancies at the metal–film interface, respectively.

It is important to note that reactions 3a and 3b, related with the formation of oxygen and hydroxyl vacancies at the metal–film interface, are represented in parallel way (refer to Fig. 1). However, it seems that exist a mutual relationship in the formation of these point defects. First, the dehydration process given by reaction 8 (Fig. 1), occurring at the *m*/*f* interface, provokes the consumption of the electrons generated by reaction 3a and the subsequent formation of atomic and/or molecular hydrogen. In these specific "sites" is reached a depletion of the hydroxyl ions concentration, consequently a diffusive process of the hydroxyl ions arises through the passive film. Under this condition, the diffusion gradient is influenced by the transfer process of reaction 8 and relies on the kinetic constant of the oxygen vacancies formation (k_{3a}). Therefore, the transfer function (Eq. (2)) arising from reactions 3a and 3b are added together, as if they occur in series.

$$Z_f = R_{1,O^{2-}}\left[1 + k_{-3a}\frac{e^{-\gamma_O L}(K+\gamma_O) - e^{\gamma_O L}(K-\gamma_O)}{j\omega(e^{\gamma_O L} - e^{-\gamma_O L})}\right] + R_{2,OH^-}\left[1 + k_{-3b}\frac{e^{-\gamma_h L/2}(K+\gamma_h) - e^{\gamma_h L/2}(K-\gamma_h)}{2j\omega(e^{\gamma_h L/2} - e^{-\gamma_h L/2})}\right] \tag{3}$$

$$\frac{1}{R_{1,O^{2-}}} = 2F(b_{3a}k_{3a} + b_{-3a}k_{-3a}C_O^0)a_1 \tag{4}$$

$$\frac{1}{R_{2,OH^-}} = F(b_{3b}k_{3b} + b_{-3b}k_{-3b}C_{OH}^0)a_1 \tag{5}$$

where $\gamma_O = \sqrt{K^2 + j\omega/D_{VO^{\cdot\cdot}}}$, $\gamma_h = \sqrt{K^2 + 4j\omega/D_{VOH^{\cdot}}}$. k_{-3a} and k_{-3b} are the backward rate constants, corresponding to the formation of both oxygen and hydroxyl vacancies (Fig. 1, reactions 3a and 3b). a_1 is the part of the potential consumed as a potential drop at the metal–film interface. The resistive terms $R_{1,O^{2-}}$ and R_{2,OH^-} involve forward and backward rate constants (reactions 3a and 3b), which do not dependent on the frequency. $D_{VO^{\cdot\cdot}}$ and $D_{VOH^{\cdot}}$ are the diffusion coefficients of the oxygen and hydroxyl vacancies. K is a constant parameter, given by $K = \varepsilon F/RT$, where ε is the electric field strength; F, the Faraday constant; R, the universal gas constant, and T, the temperature.

This model has been previously used to describe the passive properties of nickel and titanium oxides films (*p*- and *n*-type semiconductor, respectively) in borate media (pH 7–8) [18]. In this paper, it was observed that the model fits accurately the electrochemical behavior of these films. To extend the application of this model, evaluating the contribution of hydroxyl ion concentration using EIS technique was impeded, because NiO and TiO_2 are subjects of an accelerated dissolution process at higher hydroxyl concentrations. Therefore, in order to understand more the *n*-type semiconductor oxides' behavior and the phenomena involved and controlling their growth, different passive films were formed and characterized on tantalum and niobium electrodes in 0.1 M KOH solution. These oxides are known to tolerate high acidic or alkaline environments. Experimental EIS spectra were analyzed and fitted by means of a modified point defect model (PDM) previously reported by our research group [18].

2. Experimental

A conventional three-electrode cell (100 mL) was used for the measurements. Tantalum and niobium rods (Alfa AESAR™; purity 99.9%) covered with a resin and embedded in Teflon were used to generate a rotating disk working electrodes (WE), with 0.177 and 0.312 cm^2 of exposed area, respectively. A graphite rod (Alfa AESAR™, 99.999%) was utilized as the counter electrode and a Hg/Hg_2O/0.1 M KOH electrode (154 mV vs. standard hydrogen electrode) as the reference. All potentials in this work are referred to this scale. The experiments were carried out in a 0.1 M KOH (Merck™ analytic reagent) solution at pH 13. All the solutions were freshly prepared using ultrapure water (18.2 M cm, Millipore™), previously boiled in order to eliminate the carbon dioxide.

Prior to each experiment, the working electrode surface was mechanically polished, with P2000 abrasive paper to a mirror finish, using Buehler™ alumina powder (final granulometry ≤0.05 μm), rinsed with ultrapure water and placed in an ultrasonic cleaner to ensure a reproducible surface in every experiment. Ta_2O_5 and Nb_2O_5 films were electrochemically formed by one potentiostatic step imposed on the working electrode (WE), at different formation potentials (E_F) for 12 h. A steady-state current was already reached at that time. EIS spectra were acquired afterward; sweeping the frequency from 100 kHz to 63.4 mHz at 10 points per decade that is more than adequate for the system being studied. We have chosen the potentiostatic mode for the EIS technique because it yields a more defined and reproducible spectrum in the low frequency region than does the galvanostatic mode. In general, EIS experiments were performed after assessing the appropriate regions to study the kinetic of the electrochemical reactions with a *dc* technique (i.e. voltammetry). Thus, when a potentiostatic mode is used, there is a better selectivity of this region when compared with a galvanostatic experiment. Moreover, it is more probable that the wave amplitude in the galvanostatic mode is exceeded by external noise at low frequencies than in the potentiostatic. If higher amplitude modes are used in the former mode, linearization of the response of the system to the input signal is not

Download English Version:

https://daneshyari.com/en/article/220052

Download Persian Version:

https://daneshyari.com/article/220052

Daneshyari.com